Published in final edited form as:

Nature. 2015 April 2; 520(7545): 51–56. doi:10.1038/nature14186.

Loss of delta catenin function in severe autism

Tychele N. Turner[1,2,3], **Kamal Sharma**[4], **Edwin C. Oh**[5], **Yangfan P. Liu**[5], **Ryan L. Collins**[6], **Maria X. Sosa**[1,3], **Dallas R. Auer**[1,3], **Harrison Brand**[6,7], **Stephan J. Sanders**[3,8], **Daniel Moreno-De-Luca**[3,9], **Vasyl Pihur**[1,3], **Teri Plona**[10], **Kristen Pike**[10], **Daniel R. Soppet**[10], **Michael W. Smith**[11], **Sau Wai Cheung**[12], **Christa Lese Martin**[3,13], **Matthew W. State**[3,8], **Michael E. Talkowski**[6,7], **Edwin Cook**[14], **Richard Huganir**[4], **Nicholas Katsanis**[5], and **Aravinda Chakravarti**[1,3]

[1]Center for Complex Disease Genomics, Johns Hopkins University School of Medicine, Baltimore, MD, 21205 USA

[2]Predoctoral Training Program in Human Genetics and Molecular Biology, McKusick-Nathans Institute of Genetic Medicine, Johns Hopkins University School of Medicine, Baltimore, MD, 21205 USA

[3]National Institute of Mental Health (NIMH) Autism Centers of Excellence (ACE) Genetics Consortium

[4]Solomon H. Snyder Department of Neuroscience, Johns Hopkins University School of Medicine, Baltimore, MD, 21205 USA

[5]Center for Human Disease Modeling, Duke University, Durham, NC, 27710, USA

[6]Center for Human Genetic Research, Massachusetts General Hospital and Harvard Medical School, Boston, MA, 02114 USA

[7]Department of Neurology, Massachusetts General Hospital and Harvard Medical School, Boston, MA, 02114 USA

[8]Department of Psychiatry, University of California, San Francisco, San Francisco, CA 94158, USA

Send all correspondence to: Aravinda Chakravarti, Ph.D., Center for Complex Disease Genomics, McKusick-Nathans Institute of Genetic Medicine, Johns Hopkins University School of Medicine, 733 N. Broadway, BRB Suite 579, Baltimore, MD 21205, T: (410) 502-7525, F: (410) 502-7544, aravinda@jhmi.edu.

SUPPLEMENTAL INFORMATION

Supplementary information is at www.nature.com/nature

AUTHOR CONTRIBUTIONS

Designed the study and wrote the manuscript (T.T., A.C.); edited manuscript (all authors); examined phenotype data for the female autism patients (T.T., E.C.); *MECP2*/*CTNND2* sequencing and TaqMan genotyping (T.T., M.X.S., T.P., K.P., D.S., M.W.S.,); autism exome sequencing (T.T.); Simons exome sequencing analysis (S.S., M.S.); CNV analysis (S.W.C., C.L.M., D.M.D., S.S., R.C.C., H.B., M.E.T, M.S., and T.T.); *CTNND2* molecular biology (T.T., M.X.S.); zebrafish gastrulation and protein-protein interaction studies (Y.P.L., E.O., and N.K.); primary hippocampal neuron experiments and expression analysis (K.S., T.T, D.A.); bioinformatics analyses (T.T.,V.P.).

All sequence data has been deposited into the National Database for Autism Research (NDAR) and is contained within Collection 2035 (Autism Genetics, Phase II; Geschwind). Reprints and permissions information is available at www.nature.com/reprints. The authors declare no competing financial interests.

[9]Department of Psychiatry, Yale University, New Have, CT, 06511, USA

[10]Leidos Biomedical Research, Inc., Frederick, MD, 21702, USA

[11]National Human Genome Research Institute, Bethesda, MD, 20892, USA

[12]Baylor College of Medicine, Houston, TX, 77030, USA

[13]Autism & Developmental Medicine Institute, Geisinger Health System, Lewisburg, PA, 17837, USA

[14]University of Illinois at Chicago, Chicago, IL, 60608, USA

SUMMARY

Autism is a multifactorial neurodevelopmental disorder affecting more males than females; consequently, under a multifactorial genetic hypothesis, females are affected only when they cross a higher biological threshold. We hypothesize that deleterious variants at conserved residues are enriched in severely affected patients arising from FEMFs (female-enriched multiplex families) with severe disease, enhancing the detection of key autism genes in modest numbers of cases. We show the utility of this strategy by identifying missense and dosage sequence variants in the gene encoding the adhesive junction-associated delta catenin protein (*CTNND2*) in FEMFs and demonstrating their loss-of-function effect by functional analyses in zebrafish embryos and cultured hippocampal neurons from wildtype and *Ctnnd2* null mouse embryos. Finally, through gene expression and network analyses, we highlight a critical role for *CTNND2* in neuronal development and an intimate connection to chromatin biology. Our data contribute to the understanding of the genetic architecture of autism and suggest that genetic analyses of phenotypic extremes, such as FEMFs, are of innate value in multifactorial disorders.

INTRODUCTION

Autism is a common neurodevelopmental disorder with a profound sex-bias: four times as many males than females are affected[1] while disease recurrence risk to siblings of autistic females is larger than to siblings of affected males[2]. Both features can be explained through autism's multifactorial inheritance where females are affected at higher biological thresholds of an underlying liability than are males. Under this model, females escape the effect of deleterious mutations unless the alleles are severe and at key developmental steps. To accelerate discovery, we examine families with highest recurrence risk and, consequently, likely enriched for severe mutations in such genes. We hypothesize that one group of families that have this property, and yet are underrepresented in autism sequencing efforts, are those with two or more severely affected females (female-enriched multiplex families or FEMFs).

The first genes discovered in autism were through syndromes (Supplementary Table S1), such as Rett and Fragile X syndromes[3]. Today, genomic analyses have definitively identified 12 genes, from an estimated 500[4], with an excess of *de novo* or segregating mutations in typical isolated cases that are overwhelmingly male (Supplementary Table S1). Given such heterogeneity, it may be crucial to identify those genes whose mutations impart the greatest autism risk. Increased recurrence risk is associated with lower incidence

("Carter" effect), since any rare class must arise from higher genetic liability (Figure 1a)[5]. Consequently, gene discovery in epidemiologically rarer classes, namely, female gender, high phenotypic severity and familial cases, may be fruitful; this is further enhanced if we increase the genetic load by considering individuals who have all three features.

These genetically loaded cases have either a greater number or frequency of deleterious alleles that are likely severe coding variants. This prediction arises from our studies of Hirschsprung disease (HSCR), a neurodevelopment disorder (NDD) of enteric nervous system ganglionosis. HSCR is a multifactorial disorder with a sex ratio of 4:1 in favor of males and whose risk factors are gender, phenotypic severity, and familiality[6,·] Although >15 HSCR genes have been identified, the major gene encodes the receptor tyrosine kinase RET which harbors numerous rare loss-of-function coding and one common enhancer variant[7]. We estimated the proportion of 174 HSCR patients with damaging *RET* coding variants conditional on their having 3, 2, 1 or 0 risk factors, where higher risk categories were female gender, long segment aganglionosis and familiality (Figure 1b), to show that rare classes are significantly associated with a higher proportion of deleterious alleles, varying linearly between 46% and 2% from the highest to lowest risk class ($P=3.1x10^{-6}$); the non-coding variant had the reverse trend. Therefore, exome sequencing in autism can be similarly efficient in FEMFs. Since female incidence of autism is 0.0016, <10% of families are multiplex and <10% are severe, FEMFs have a crude incidence of $<1.6x10^{-5}$ and represent a rare autism disorder enriched for deleterious coding variants[7].

Here, we demonstrate the utility of this strategy by exome sequence analyses of 13 unrelated females and identifying 18 candidate genes of which at least four, *CYFIP1*, *DLG1*, *PLXNA3*, and *CTNND2*, are of interest to autism etiology. We have evaluated one of them, *CTNND2* (the delta 2 catenin gene encoding the delta catenin protein) in depth using a combination of genetic, genomic and functional studies to show that (1) *CTNND2* harbors a significant excess of deleterious missense and copy number variants in autism; (2) these variants, by functional testing, are loss-of-function and affect Wnt signaling; (3) expression of *CTNND2* is highest in the fetal brain and is highly correlated with other autism genes; and, (4) *CTNND2* correlated genes are enriched for chromatin and histone modification, as well as dendritic morphogenesis, functions. These results are consistent with the roles of CTNND2 in the formation of dendritic spines[8], and the regulation of beta catenin in neurons[9]. Given the recent finding of *de novo* autism mutations in pathways regulating beta catenin (Supplementary Table S1), loss-of-function of CTNND2 is likely rate-limiting for dendritic morphogenesis and maintenance.

RESULTS

Exome sequencing of females with autism

We sampled 13 unrelated females, negative for deleterious variants in *MECP2*, from multiplex families who had severe autism (ADI-R+ and ADOS+). Proband exomes were sequenced and analyzed with sequence data from 71 European females (1000 Genomes project (1000G); Extended Data Figure 1). To identify pathogenic alleles, we focused on missense variants absent in public databases (dbSNP129, 1000G) and conserved to zebrafish, nonsense, and canonical splice site variants. This led to 3,090 variants of interest

(VOI) in the combined 84 exomes within 2,516 genes with 447 of these having 2+ VOI; among them, the 13 autism cases harbored 2+ VOI in 24 genes and 18 of these reached significance ($P<1x10^{-4}$) (Supplementary Table S2). By searching their expression profiles (Supplementary Table S3), we identified four genes, with an excess of deleterious alleles, as candidates: *CYFIP1, DLG1, PLXNA3,* and *CTNND2*. On the basis of our previous genome-wide association study implicating chromosome 5p[10], we followed up *CTNND2* at this locus.

CTNND2 as a novel autism gene

CTNND2 harbored two deleterious variants, G34S and R713C both of which were absent in 3,889 European controls (1000G and Exome Variant Server (EVS)); G34S was present at a frequency of $5.3x10^{-4}$ in 1,869 African ancestry samples (EVS) and in one Luhyan sample (NA19020) (Extended Data Figure 2). To estimate their frequency, we genotyped 10,782 samples from the HapMap and autism collections: the only additional individuals with G34S were an affected *female* and her mother (SSC02696, SSC03276) from the Simons Simplex Collection (SSC). Principal component analysis on polymorphism data from G34S individuals found that our autism cases were not of African ancestry, identifying a new ancestral origin for G34S (Extended Data Figure 3). For R713C, only our FEMF samples were heterozygous. Next-generation *CTNND2* sequencing in 362 additional autism females (Extended Data Figures 4) identified a total of seven variants (G34S, R713C and five new variants: P189L, P224L, G275C, R454H, T862M) of which four (G34S, G275C, R713C, T862M) were conserved to zebrafish (Figure 2a, Supplementary Table S4). We also identified Q507P in an autistic male from 170 SSC probands. An identical analysis of 379 European ancestry control samples (1000G) yielded three variants after validation (R330H,D465N,A482T), one conserved to zebrafish. On aggregate, variants at these conserved CTNND2 residues are significantly more frequent in autism than in controls ($P=0.04$ vs. 1000G; $P=7.8x10^{-4}$ vs. EVS).

We next assessed whether copy number variants (CNVs) within *CTNND2* were enriched in autism. First, from the literature, we identified six deletions and one duplication. Second, we identified two deletions and one duplication from the Emory University and Baylor College of Medicine clinical cytogenetics laboratories. Third, from AGRE, we identified two previously unreported valid deletions (Extended Data Figure 5). Therefore, we detected 12 CNVs (10 deletions, 2 duplications), 7 overlapping one or more exons (Figure 3, Supplementary Table S5). As a control, we searched the Database of Genomic Variants (DGV) to identify 33 variants, with only two overlapping exons (58.3% in our 12 CNVs versus 6.1% in DGV; $P=5x10^{-4}$). This significant excess of exon-disruptive deletions suggests *CTNND2* haploinsufficiency in autism. Most of our patients had an autism diagnosis; however, some probands were referred with a diagnosis of NDD. To test whether *CTNND2* CNVs may be enriched in NDDs generally, we assessed CNVs from 19,556 independent cases referred for clinical diagnostic studies and 13,898 controls from population-based studies[11]. Considering all dosage imbalances, we observed 25 instances in cases and 3 in controls, corresponding to an odds ratio of 5.9 ($P=4.10x10^{-4}$) (Extended Data Figure 6, Supplementary Table S6). The impact of loss-of-function (deletions, unbalanced translocations) mutations at this locus is significant with an odds ratio of 14.7

($P=8.28x10^{-5}$), with specificity for *CTNND2* since the effect size is comparable for intragenic deletions (8 cases, 1 control; P=0.059, OR=5.68) as for all CNVs.

The consequence of autism variants on function

To assess the *in vivo* functional consequences of autism *CTNND2* variants, we used a complementation assay in zebrafish embryos. Zebrafish has two genes for delta catenin that are as divergent from each other (18.3%) as they are from humans (19.9%, 20.7%), at the protein level. We examined expression of both genes by RT-PCR at six developmental time points (Figure 2b) and focused on *ctnnd2b* because it was expressed at all stages. Using a splice-blocking morpholino (MO) targeting *ctnnd2b*, we injected 1–8 cell embryos and analyzed at the 8–10 somite stage. Morphant embryos had gastrulation phenotypes consistent with abnormal *Wnt* signaling (shortened body axes, longer somites, and broad and kinked notochords) (Figure 2c). RT-PCR of *axin2* mRNA, a direct target of canonical Wnt signaling[12], from 10-somite *ctnnd2b* morphants, showed significant decrease (P<0.01) reinforcing the hypothesis of defective Wnt signaling (Extended Data Figure 7a). Specificity of the MO was tested by co-injection of wild-type mRNA to observe significant (P<0.001) rescue (Figure 2d). To investigate the effect of each variant on protein function, injection cocktails containing MO and mutant variants were injected and compared to rescue with wild-type mRNA: five variants (G34S,P189L,P224L,R454H,Q507P) were better than morpholino alone (P<0.001) but worse than wild-type rescue (P<0.001), implicating these as hypomorphic (Figure 2d). One variant (R713C) was functionally null while G275C and T862M were benign, and all four controls were benign, demonstrating specificity. To preclude the possibility of mRNA toxicity, we injected mutant mRNA corresponding to all alleles and observed no significant differences in the gastrulation phenotypes (Figure 2e).

To replicate these findings with an *in vivo* assay querying Wnt signaling earlier in development, we assessed the consequences of *ctnnd2b* suppression on *chordin* expression during epiboly, whose ectopic expression is known in Wnt mutants[13]. Consistent with *chordin*'s role in Wnt-dependent dorsalization[14], we observed shortening and widening of the *chordin* expression domain as well as loss of anterior-specific expression fields in *ctnnd2b* morphants (Extended Data Figure 7b); this phenotype could be rescued by wildtype mRNA. Further, testing of two control alleles that scored benign in our mid-somitic assays (A482T, G810R) showed significant rescue (P<0.001); the hypomorphic allele G34S rescued *chordin* expression to a level significantly worse than wildtype mRNA rescue (P<0.001), while the null allele R713C did not rescue *chordin* expression (Extended Data Figure 7c). Since CTNND2 can bind CTNNB1[15], we tested this interaction with mutant CTNND2. Expression of GFP-tagged *CTNND2* and Flag-tagged *CTNNB1* revealed that wild-type CTNND2 could immunoprecipitate CTNNB1, however, its interaction with CTNNB1 was diminished upon expression of G34S or R713C (Extended Data Figure 7d), suggesting *in vivo* Wnt phenotypes may result from attenuated CTNNB1-CTNND2 interaction.

Finally, we asked if these major *CTNND2* sequence variants could affect neuronal circuitry by employing a well-established *in vitro* model system. Dendritic spines are the primary sites for excitatory synapse formation, and their dysregulation underlies many

neuropsychiatric disorders[16]. To test if *CTNND2* variants interfere with development and maintenance of spines, we prepared primary hippocampal neurons from E18 rat embryos and introduced either GFP or GFP fusion to wild type *CTNND2* or to its mutant variants at DIV8. At DIV15, neurons were fixed and analyzed to assess spine density. We found that wild type *CTNND2* had a significantly higher spine density versus GFP controls[17]. However, neurons expressing G34S had a significantly lower spine density than those expressing GFP or wild type *CTNND2*. Neurons expressing R713C on the other hand had the same spine density as those expressing GFP but significantly less than the one that expressed wild type *CTNND2*, suggesting a loss-of-function effect. In contrast, the A482T polymorphism had an effect similar to wild type CTNND2 (Extended Data Figure 8). To test if observed changes in spine density reflected changes in excitatory synapse number in the networks, we analyzed excitatory synapses i.e. overlapping region between postsynaptic marker PSD95 and presynaptic marker vGluT1 in mouse hippocampal neurons at DIV14 (Figure 4a). As with spine density, we found an increase in excitatory synapse number in neurons that overexpress wild type but not mutant CTNND2. Further, loss-of-function of CTNND2 led to a decrease in overall excitatory synapse density, as well as active synapses that express the GluA subunit of the AMPA type glutamate receptors (Figure 4b, 4c). Taken together, these results suggest that CTNND2 is critical to the formation and/or maintenance of synapses, in accord with other studies[18,19]. Moreover, unlike wild type CTNND2, the tested mutants failed to rescue the reduction in synapse density in CTNND2 null background, demonstrating loss-of-function. Therefore, G34S and R713C impair development and/or the maintenance of mammalian neural circuitry.

Expression of CTNND2 in the developing human brain

To understand *CTNND2* expression, we tested mRNA levels in 16 adult and eight fetal human tissues: *CTNND2* expression was highest in the fetal brain (20x the adult brain) (Extended Data Figure 9). Therefore, we used the Allen Brain Atlas Developing Human Brain microarray data to identify other *CTNND2* co-expressed genes. We used the data normalized to 17,630 genes and linear regression on age and brain regions for estimating Pearsonian correlations between *CTNND2* and all other genes (absolute correlation >0.3, $P=2.84x10^{-6}$ given multiple comparisons). First, we performed pathway analysis on the 826 positively and 662 negatively correlated genes (Supplementary Table S7). The positive set was significantly enriched for genes encoding proteins localized to the cytoskeleton, cell junction, neuronal projection, with GTPase regulatory activity, and functioning in cell morphogenesis, chromatin modification, neuronal development and neuron projection formation. Of these, CTNND2's role in dendritic development and spine morphogenesis is known[17] as well as its involvement in actin dynamics and GTPase regulatory activity[20,21]. However, its role in chromatin modification is novel. The closest known function of CTNND2 to chromatin is based on CTNND2 binding to ZBTB33[22], a protein regulating transcription and *Wnt* pathway genes[23], and its possible nuclear localization and function[24]. Second, we searched for transcription factors that may regulate *CTNND2:* among the correlated genes we identified 75 of which PAX6 is the most biologically significant.[25] A *Pax6* mutant rat show autism-related features[26] and genetic variation disrupting *PAX6* has been identified in individuals with autism[27]. Also, Pax6 can regulate *Ctnnd2* expression in cells, including the binding of Pax6 to its promoter.[25,28]

We searched the correlated genes for autism[29] (https://gene.sfari.org/autdb/) and intellectual disability candidates (Supplementary Table S7). Of 529 autism genes, 71 (61 positively, 10 negatively) were significantly correlated with *CTNND2*, representing significant enrichment ($P=2.83x10^{-6}$). Next, we examined the correlations between these 71 genes and *CTNND2* (Figure 5a) to find an intimate relationship between CTNND2 and autism genes. To interrogate the function of the 61 positively correlated genes, we again performed pathway analyses (Figure 5b) to find significant enrichment of genes involved in dendrite morphogenesis ($P=2.96x10^{-3}$; *PDLIM5,MAP2,SHANK1,CDKL5,DLG4*) as well in chromatin modification ($P=2.96x10^{-3}$; *HDAC3,HUWE1,CREBBP,EP300,YEATS2,EP400, ATXN7,HCFC1 ARID1B,NSD1*).

DISCUSSION

Our studies strongly implicate delta-2 catenin (*CTNND2*) as a critical gene in autism and an important neurodevelopmental protein given its role in FEMFs, functional association with other autism genes, Cri-du-chat syndrome[30] and other diseases[31]. Clearly, *CTNND2* haploinsufficiency is common in autism and strongly associated with NDD generally. Nevertheless, in the general population, the frequency of disease alleles we discovered is low ($3.9x10^{-4}$ and $8.0x10^{-4}$ in individuals of European and African ancestry, respectively, in EVS), consistent with their deleterious functional effects.

CTNND2 is a plakoglobin/armadillo family member with identity to PKP4, CTNND1, and ARVCF. The armadillo domain is a key part of the protein that binds cadherins[15], beta-catenin[15], presenilins 1 and 2[32], and sphingosine kinase[33]. It also harbors a coiled-coil domain, a polyproline tract at amino acids 219-224 where src receptor kinases bind[34], and a PDZ domain at the C-terminus, which can bind Discs large homolog 4[35] and erbin[36]. These features suggest that CTNND2 is important in neuronal actin dynamics and the cytoskeleton[15,34], as also supported by observations of induced branching of dendrite-like processes and enhanced dendrite morphogenesis by CTNND2 overexpression[37]. Importantly, CTNND2 can directly bind to actin[37] and cortactin[34], and act on the Rho family to induce filopidia within neurons[20] and increase the number of dendritic spines[17]. Finally, we demonstrate a role of CTNND2 in canonical *Wnt* signaling through zebrafish analyses: although the precise mechanism is not understood, it can bind to proteins (GSK-3β, ZBTB33) that regulate *Wnt* signaling[23] and transcription[22], in concert with CTNNB1. The other novel CTNND2 function we implicate is its possible role in the nucleus, through its interaction with HDAC3 (Figure 5). This is not unexpected, since CTNND2 can affect gene expression after nuclear translocation[24]. Furthermore, the armadillo family member p120ctn interacts with ZBTB33 (Kaiso) and the NCoR co-repressor complex containing HDAC3[22,24,38,39]. Thus, we hypothesize that CTNND2 maybe a nucleo-cytoplasmic protein whose autism effect may arise from its cytoplasmic or nuclear loss-of-function or both.

Published *Ctnnd2* knock-out mice[8,18,19], and our analyses of their dendritic spines, give clues to the role of *CTNND2* in autism and in cognition. Homozygote mice exhibit structural and functional abnormalities at the synapse, as well as impaired spatial learning and fear conditioning[18,19], with reduced levels of PSD-95, beta catenin associated with cadherin, and

N-cadherin. PSD-95's interaction with CTNND2 was discovered as an important linkage to AMPA receptor binding protein and GRIP[35]. Our results confirm that CTNND2 is required for the maintenance of spine structures *in vivo*[19], and stability of some key components of the synaptogenic machinery such as N-Cadherins and PSD95[8,18]. We show that loss of spines and reduction in total levels of synaptic proteins in null mice reflects reduction in the number of functional excitatory synapses at the subcellular level. Interestingly, acute loss of delta catenin *in vitro* impairs activity-dependent formation of spines[40], reinforcing the importance of delta catenin in formation and maintenance of synaptic structures and cognitive functions.

Studying FEMFs is unconventional for a complex disease where most mutations have small effects. Nevertheless, our data suggests that modest numbers of samples of *rare extreme* phenotypes, in contrast to large numbers of *typical* cases, can be important. Note, we identified 18 candidate genes among which at least three others are worthy of follow-up: *CYFIP1* is in a 15q11-13 autism duplication, has altered expression in autism patients, interacts with FMRP, and is involved in regulating dendritic spines through translational inhibition and actin dynamics[41]; *DLG1* is a multi-scaffolding post-synaptic density protein lying within a 3q29 autism and/or intellectual disability deletion; *PLXNA3* is known to alter dendritic spines and is a receptor for *SEMA5A*[42], another autism gene[10]. The broader FEMFs hypothesis can thus be tested by sequencing larger numbers of cases for identifying genes critical to early brain development.

METHODS

Human subjects and animal experiment permissions

We studied 13 unrelated females, 12 from FEMFs and one from a family with an affected girl and boy, from the Autism Genetic Resource Exchange (AGRE)[43] and the National Institute of Mental Health (NIMH) collections (www.nimhgenetics.org). Of these, 11 were of European, one each of Hispanic and Native Hawaiian or Pacific island ancestry. Human subject studies were approved by the Johns Hopkins Medicine Institutional Review Board (IRB NA_00015748). All protocols for animal care, use and euthanasia were reviewed and approved by the Institutional Animal Care and Use Committees of Johns Hopkins University (Protocol MO12M412) and Duke University (Protocol A229-12-08), and were in accordance with the Association for Assessment and Accreditation of Laboratory Animal Care (AAALAC) guidelines.

DNA Sequencing

MECP2 sequencing—Each of the 13 autism individuals was assessed for the *4* coding exons of *MECP2* by PCR amplification of each exon and Sanger sequencing, performed at Beckman Coulter Genomics. The sequence traces were analyzed in Sequencher version 4.7.

Exome sequencing & read mapping—We analyzed 10 female autism cases and 1 HapMap sample (NA18507) utilizing the Agilent SureSelect Whole Exome capture (38 megabases) and SOLiD 3+ and 4 technologies. For 3 additional female autism individuals, sequencing used the Illumina TruSeq Whole Exome capture (62 megabases) and Illumina

technology; all Illumina exome experimental steps were performed at the Illumina sequencing center (Hayward, CA). The SOLiD and Illumina data were mapped to the human genome build 37 using the BFAST[44] and BWA[45] programs, respectively. Subsequently, the SAM output was converted to BAM output, duplicates were marked using Picard, and indel realignment and quality score recalibration were performed in GATK[46]. Variants were called across all exomes as well as 71 of the 1000 Genomes European female exomes. Each variant was annotated for genetic features using ANNOVAR[47]. Additional annotations included presence in 1000 Genomes, conservation to zebrafish, and presence in autism, autism candidate, or intellectual disability genes based on the published literature (Pinto et al. 2010[29] and https://gene.sfari.org/autdb/). In total, we identified 37,424 non-synonymous, 486 stop gain, 32 stop loss, 35,549 synonymous, and 273 splice variants.

CTNND2 sequencing & read mapping—362 females with autism (300 unrelated, independent), 10 HapMap samples and a pooled individual sample replicated 8 times were sequenced for all of *CTNND2* coding exons. To amplify the 22 RefSeq exons and 7 Ensembl exons in *CTNND2*, 87 amplicons were designed on the Fluidigm Access Array Targeted Resequencing platform. Amplification and addition of barcodes were accomplished as described in the manual using the bidirectional sequencing primer strategy. Next, each sample was purified using Agencourt AMPure beads following the manufacturer's protocol. All samples were run on Agilent High Sensitivity DNA Chips on the Agilent 2100 Bioanalyzer to confirm size range and purity of the PCR product, followed by qPCR for quantification before pooling all 384 samples for sequencing. The library was sequenced on a single lane of the Illumina HiSeq (100 base, single pass reads) instrument following the Illumina Sequencing Strategy as described in the Fluidigm Access Array manual. Each sample fastq read was assigned and partitioned to an amplicon based on its primer sequence using *sabre* (https://github.com/ucdavis-bioinformatics/sabre), and then aligned only to that amplicon using BWA. All the resulting sam files for each individual were combined using Picard into 1 sample bam. Variants were called per individual using GATK and hard filters to get high-quality variants. To assess genotype quality of the HapMap samples, comparisons were made to HapMap genotype, OMNI genotype and 1000 Genomes data. The pooled individual replicate was also utilized for data quality control (QC).

Variant validation—All *CTNND2* missense changes identified were sequenced by Sanger chemistry for validation. Primers were designed to cover the exons in which the variants were found. A portion of each PCR product was run on a 1.8% agarose gel for 1.5 hours to check for the expected product size. Upon confirmation, the rest of the product underwent PCR purification. The purified samples were quantified by nanodrop, diluted to 25ng/μl and sent to Beckman Coulter Genomics for Sanger sequencing. Subsequently, the reads were analyzed in Sequencher version 4.7

Genotyping

CTNND2 TaqMan assay for the G34S and R713C variants—To test the frequency of the 2 *CTNND2* variants we found in the autism exomes we utilized TaqMan genotyping and created synthetic homozygous reference/mutant genotypes within a plasmid containing DNA from our patients, and also used the patient DNA on each plate as a heterozygous

control, to ensure that we would get 3 cluster plots in the SDS software. We ran a total of 11,788 reactions including 1,006 duplicates for which there was 100% genotype concordance. To genotype the G34S and R713C variants custom TaqMan genotyping assays were designed for each variant.

Principal Component Analysis for Ancestry

The 5 individuals (03C16092, 03C16094, SSC02696, SSC03276, NA19020) containing the G34S variant were assessed for ancestry by Principal Component Analysis. A set of ~6,000 autosomal SNPs genotyped in common in all 5 samples (Affymetrix 5.0, Affymetrix 5.0, Illumina 1MDuo, Illumina 1MDuo, Illumina OMNI 2.5) were analyzed using the Eigenstrat program. Genotypes from reference populations came from the CEU, YRI, and CHB/JPT populations.

Copy Number Validation

TaqMan Copy Number Assays were used for validation of CNVs in the AGRE samples (AU066818, AU075604, AU1178301, AU051503) and their family members. 3–4 assays were run for each CNV region in each sample. NA10836 was used a calibration sample in the CopyCaller Software v2.0 for a copy number of 2 in each region.

Phylogenetic Analysis

After alignment with ClustalW, Molecular Evolutionary Genetics Analysis (MEGA) software was utilized for generating a phylogenetic tree by the neighbor-joining method; a total of 1,163 and 678 positions were used to assess % identity for orthologs and paralogs, respectively.

Statistical Analysis

Exome sequence—This study focused on “variants of interest” (VOI) defined as those that were absent in both dbsnp129 and 1000 Genomes low-pass sequencing data and were likely functionally deleterious (missense at residues conserved to zebrafish (human, chimp, dog, cow, mouse, rat and zebrafish from the UCSC 46 way alignment), nonsense, and canonical splice site changes). We compared each gene and its number of VOI with that expected based on 10,000 replications of random sampling of 13 exomes from 71 female European controls. Genes having 2+ VOI only in autism exomes were considered to be relevant candidates.

Allen Brain Atlas Data—The Allen Brain Atlas Microarray (Affymetrix Human Exon 1.0 ST data microarray summarized to genes (n=17,630 genes)) dataset for the Developing Human Brain (8 post-conception weeks (pcw) to 40 years) was downloaded from the Allen Brain Atlas website on February 24, 2012. Linear regression was performed on the dataset for age and brain region (in R software). Pearsonian correlations were calculated for each gene (X) and *CTNND2* (Y) and genes with absolute values > 0.3 were retained, corresponding to an experiment-wise P=0.05 (17,630 comparisons) significance level. Pathway analyses were performed using GeneMania (www.genemania.org). DAVID analysis was performed on all correlated genes using the following categories: GOTERMs

(biological process, cellular compartment, and molecular function) for function and UCSC TFBS.

Functional Assays

Generation of human CTNND2 and mouse Ctnnd2 constructs—Human *CTNND2* was initially cloned into the pDONR221 Gateway vector. Subsequently, the human DNA was cloned into the pCS2 vector for zebrafish assays and pcDNA 6.2 N-EmGFP-DEST vector (Gateway) for the neuronal assays.

Zebrafish Gastrulation Assays—Using a splice-blocking morpholino (MO) targeting zebrafish *ctnnd2*, 1–8 cell stage embryos were injected (N=50–180) and live embryos at the 8–10 somite stage were analyzed for gastrulation phenotypes including shortened body axes, longer somites, and broad and kinked notochords in morphant embryos. Embryos with phenotypes were then classified as class I or II depending on their severity (features of the convergence/extension phenotype include a shortened body axis, wider somites, and a kinked notochord with class I having 1–2 and class II having all 3 of these components, respectively). Specificity of the morpholino reagent was tested by co-injection of wild-type human *CTNND2* mRNA. To test *CTNND2* variants, injection cocktails containing MO and mutant human *CTNND2* variants were injected and compared to the rescue condition of wild-type human *CTNND2*.

Zebrafish Chordin Expression Assay—Zebrafish embryos were harvested at 90% epiboly stage and fixed in 4% Paraformaldehyde at 4°C. Whole-mount RNA *in situ* hybridization was performed with a digoxigenin-labeled anti-*chordin* RNA probe synthesized by *in vitro* transcription (Roche). The *chordin* expression domain was measured in lateral view (“L” in Extended Data Figure 7b). The middle point of the expression domain length and the center of the embryo was linked with a dashed line (Extended Data Figure 7b), along which the width of *chordin* expression domain (“W” in Extended Data Figure 7b) was measured. Length/width ratio was calculated to quantify ectopic expression.

Immunoblotting—Cells were transfected with *CTNND2* and *CTNNB1* expression constructs and harvested 48 hours later. Protein lysates were immunoprecipitated using an anti-GFP antibody (Roche 11814460001) and immunoblotted with an anti-Flag antibody (Sigma F7425).

Neuronal Cultures and Synapse analysis—Hippocampi from day E18 rats or E17 mouse embryos were prepared and maintained as described elsewhere[48]. At day *in vitro* 8 (DIV8), the cells were transfected with GFP constructs (pcDNA6.2/N-EmGFP-DEST: alone, fused to wild type or variant allele containing *CTNND2*) and 500 ng of pCAG-DsRed2 using Lipofectamine 2000 (Life Technologies). On DIV16, cells were fixed with a 4% paraformaldehyde/4% sucrose solution, followed by immunolabeling with primary antibodies against the appropriate target as described and their respective secondary antibodies. Neurons were imaged either on a Zeiss 510 confocal for spine analysis or on Zeiss epifluorescence microscope for synapse analysis, and analyzed using ImageJ. Synapses were defined as puncta with overlapping signal between vGluT1 (Millipore Cat.

No. AB5905) and PSD95 (K28/43 clone from Neuromab) or vGluT1 and GluA (Polyclonal antibody raised in rabbit against C-Terminus of GluA subunit). To assess the expression of transfected CTNND2 and its mutant alleles in the delta catenin null background, we selected 5 pre-defined areas of interest with constant area in each dendrite (Extended Data Figure 10).

Gene Expression Assays

Expression of ctnnd2a and ctnnd2b in zebrafish—To assess mRNA expression of the two zebrafish orthologs (*ctnnd2a*, *ctnnd2b*) of human delta catenin we performed PCR on normalized cDNA libraries (gift of Dr. Samantha Maragh) from zebrafish at various developmental stages (50% epiboly, 75% epiboly, bud, 13 somite, 24 hours post fertilization, and 3 days).

CTNND2 expression analysis in human and mouse tissues—To examine expression of *CTNND2* in different human tissues the Human MTC cDNA Panel 1 (Clontech Catalog #636742, Lot #7080213), Human MTC cDNA Panel II (Clontech Catalog #636743, Lot #6040176), and the Human Fetal MTC cDNA Panel (Catalog #636747, Lot #5090557) were analyzed by a TaqMan gene expression assay (Catalog #Hs00181643_m1) for *CTNND2* and also for a pipetting control (*GAPDH*, Catalog # 4333764T). Each tissue was tested in triplicate. Subsequently, the Ct values were averaged and the ΔCt calculated between all of the tissues and the adult brain. The fold difference from brain was calculated as $(1/(2^{\Delta Ct}))$ for each tissue.

Extended Data

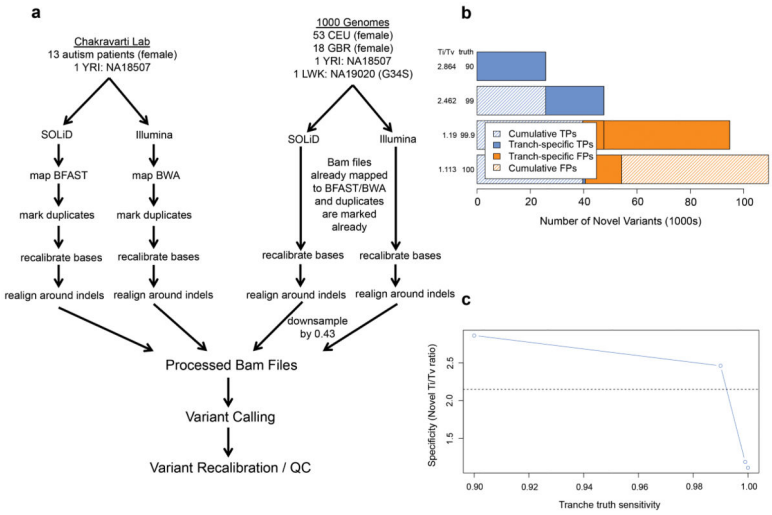

Extended Data Figure 1.

(a) Workflow of exome analysis in this study. (b) Variant recalibration metrics exhibiting why a 99% cutoff was utilized for truth sensitivity. (c) Variant recalibration specificity vs. sensitivity.

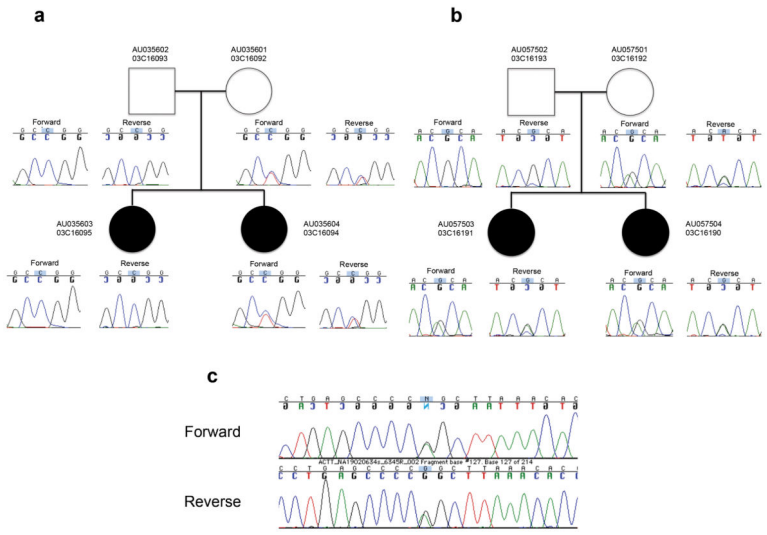

Extended Data Figure 2.
Sanger sequencing chromatograms for (a) G34S variant in this study; (b) R713C variants in this study; (c) R713C in NA19020.

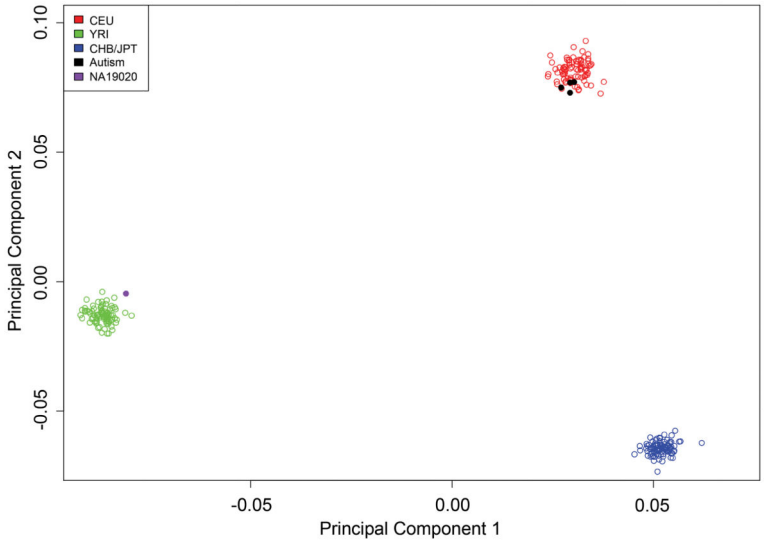

Extended Data Figure 3.
Principal components analysis of 6,211 shared autosomal SNPs in CEU, YRI, CHB/JPT, autism and NA19020 samples.

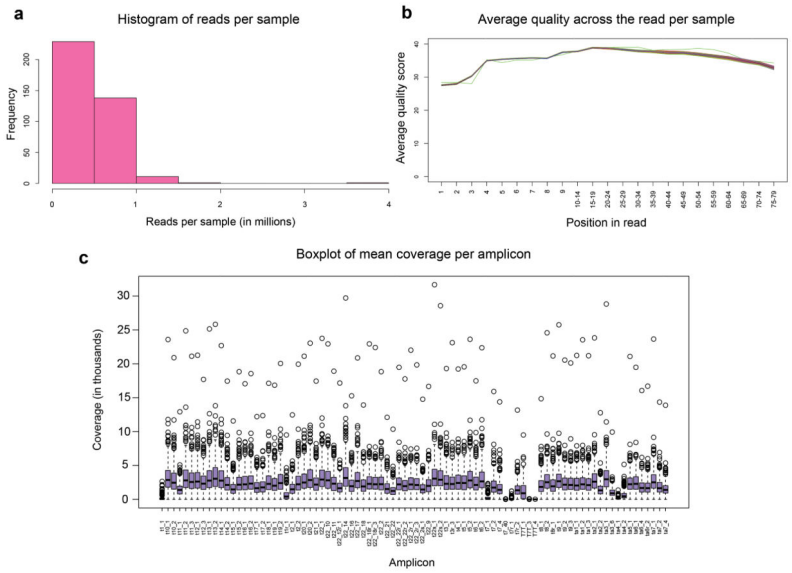

Extended Data Figure 4.
Read and Amplicon Metrics in *CTNND2* Sequencing. (a) Histogram of Reads per Sample; (b) Average quality scores across the read across all samples with each sample represented by a separate line; (c) Boxplot of Coverage per Amplicon.

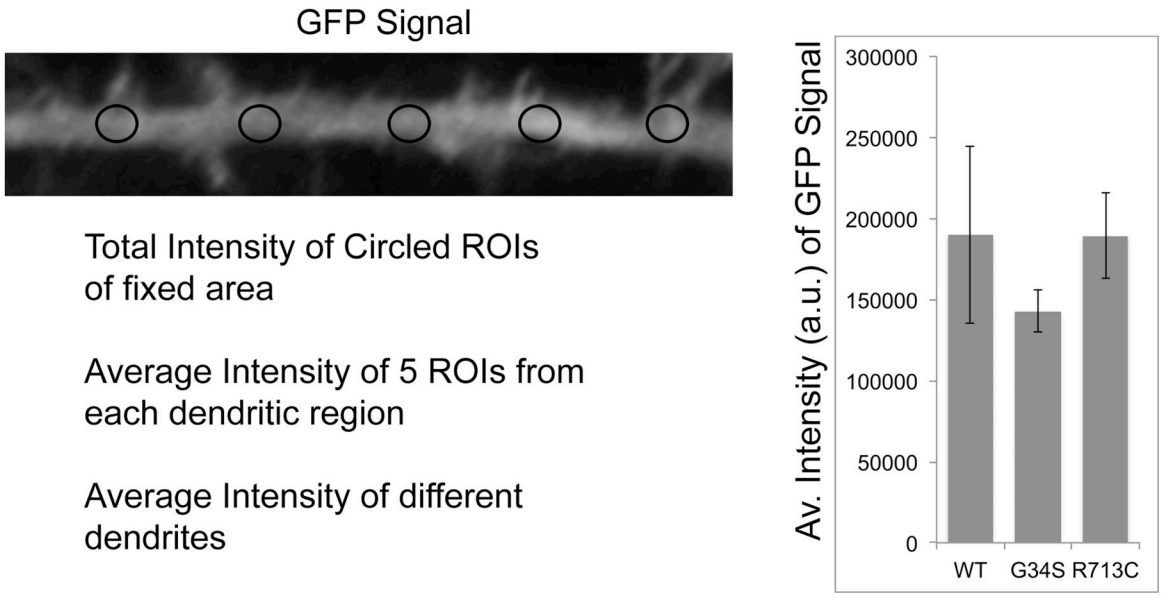

Extended Data Figure 5.
Validation of deletions in (a) AU066818, (b) AU075604, (c) AU1178301 and AU1178202, (d) AU051503.

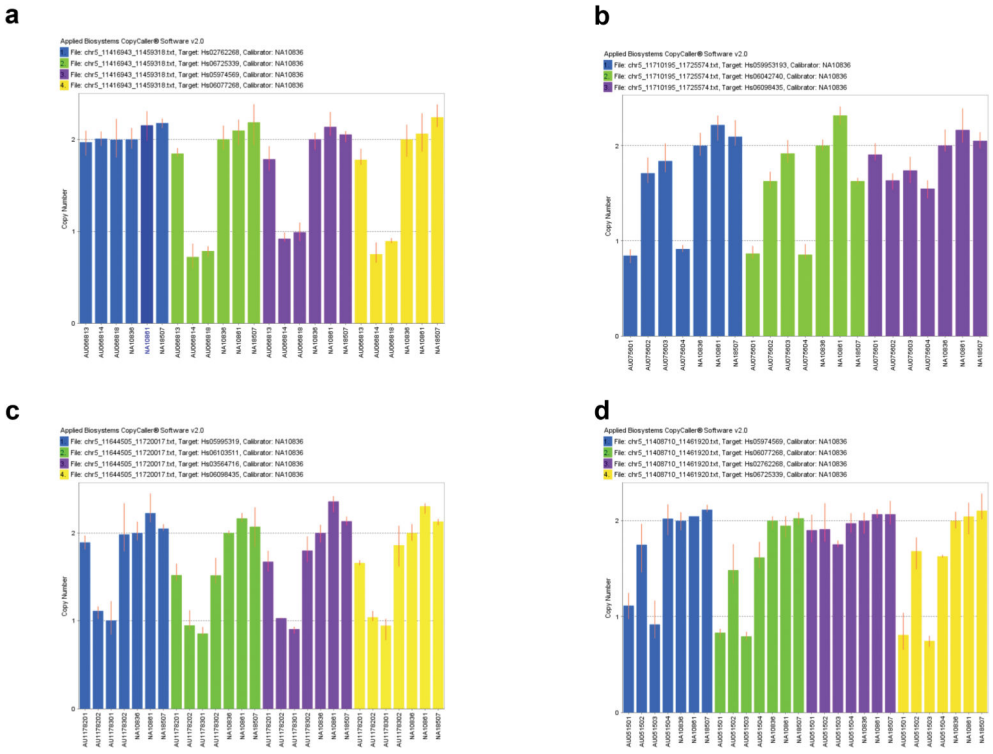

Extended Data Figure 6.
CTNND2 copy number variants from patients with neurodevelopment disorders (NDD) studied using methods published in Talkowski et al. (2012).

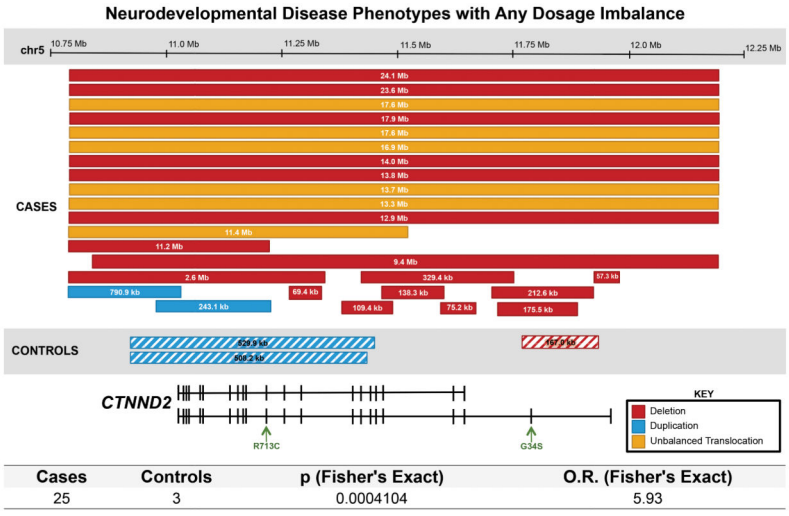

Extended Data Figure 7.
Wnt defects in ctnnd2b zebrafish morphant embryos. (a) Relative *axin2* mRNA level in 10-somite stage in control vs. morphant embryos. (b) Whole mount RNA *in situ* hybridization of *chordin*. Dorsal view in upper panels with the anterior aspect at the apex. The dorsal axis is marked with a red dashed line and regions with high expression are marked (arrows) in

control embryos. Lateral view in lower panels, length (L) and width (W) of *chordin* expression domains were measured. (c) Quantification of *chordin* expression domains (length/width ratio) in injected embryos. (d) Immunoblot showing a macromolecular interaction between Flag-tagged CTNNB1 and GFP-tagged CTNND2 with the corresponding variants. Two-sided *t*-tests were conducted with *, ** and *** indicating P < 0.05, P < 0.01 and P < 0.001, respectively. Sample size (n) is marked for each condition.

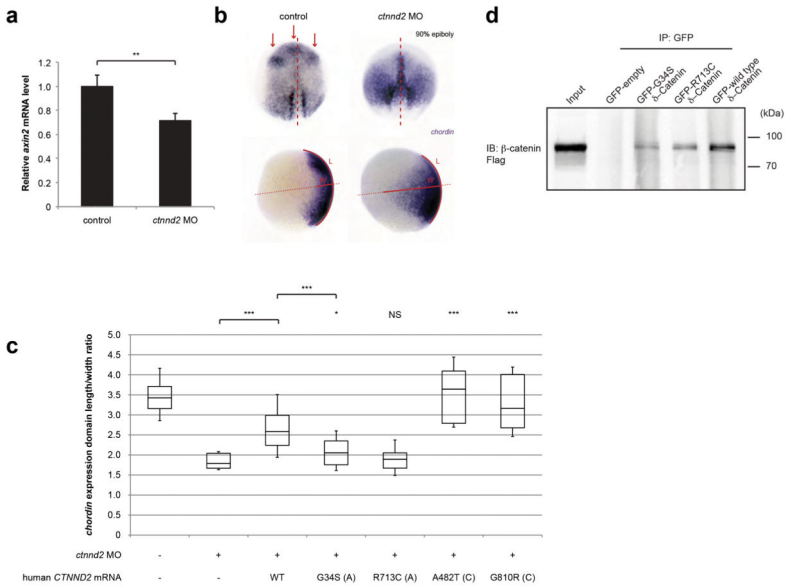

Extended Data Figure 8.

Functional in vitro modeling of delta catenin missense variants in embryonic rat hippocampal neurons. (a) Representation of spines along the dendrite in control and overexpression GFP vectors (empty or fused with wild type or variant allele containing CTNND2 (G34S, R713C, A482T (control)). Cell counts for each construct were as follows: GFP (N=32), GFP-WT (N=27), GFP-G34S (N=29), GFP-R713C (N=26), and GFP-A482T (N=29). (b) Quantification of dendritic spine numbers and statistical comparisons by Tukey's Honestly Significant test following ANOVA. * and ** both indicate P<0.05 than GFP and significantly different than wild type, respectively.

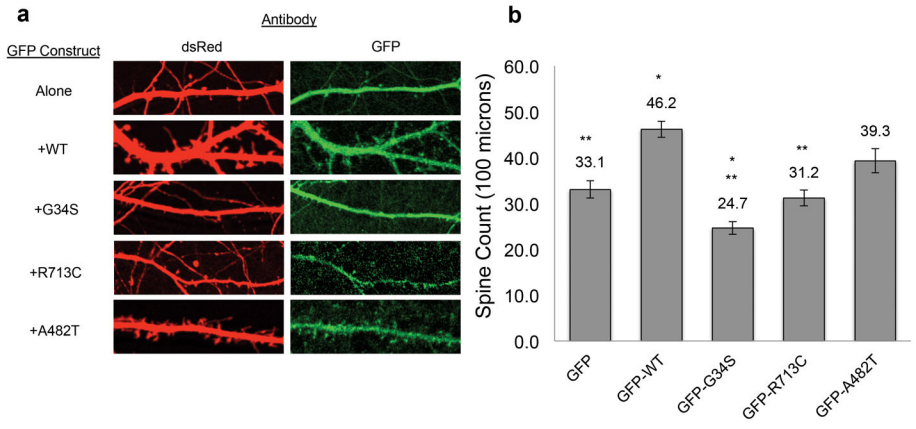

Extended Data Figure 9.

Gene expression of CTNND2 and co-expression with known autism genes. (a) Expression of *CTNND2* in various human fetal and adult tissues, shown as fold difference relative to adult brain. (b) RNA-Seq-based *CTNND2* gene expression in the developing human brain (www.brainspan.org); shown are log2RPKM expression values at time-points from 8 post-conception weeks to 40 years of age, with the lowest to highest expression colored from navy blue to red. Controls for high expression, low to no expression and known autism genes are *GAPDH*, *CFTR*, and *MECP2*, respectively.

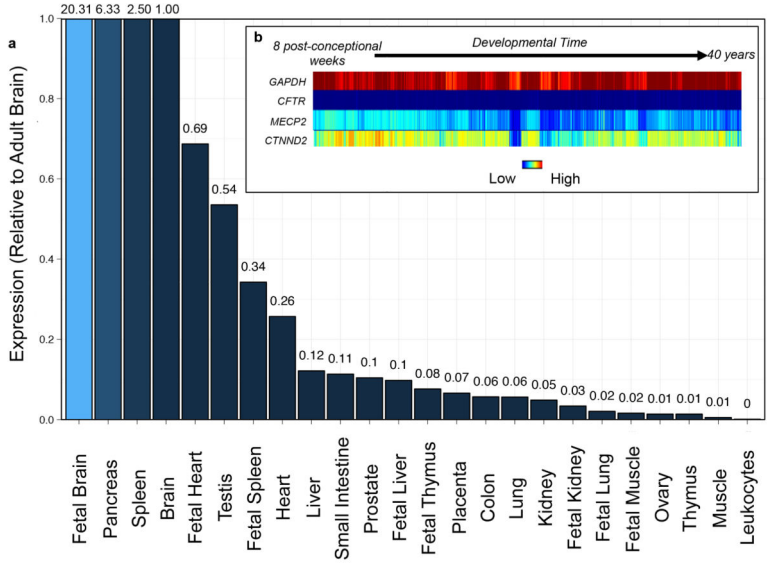

Extended Data Figure 10.

Analysis of overexpression of transiently transfected neurons: Representation of average intensity of 5 individual ROIs from a selected dendritic region. Quantitative comparison does not reveal a significant difference in expression levels of different variants of *CTNND2*.

Supplementary Material

Refer to Web version on PubMed Central for supplementary material.

Acknowledgments

We wish to acknowledge the participation of all of the families in the AGRE, NIMH, and SSC studies that have been a model of public participatory research. The Autism Genetic Resource Exchange (AGRE) is a program of Autism Speaks and is supported, in part, by grant 1U24MH081810 from the National Institute of Mental Health to Clara M. Lajonchere (PI). The SFARI Simplex Collection (SSC) used here was developed by the following principal investigators: A. Beaudet, R. Bernier, J. Constantino, E. Cook, E. Fombonne, D. Geschwind, D. Grice, A. Klin, D. Ledbetter, C. Lord, C. Martin, D. Martin, R. Maxim, J. Miles, O. Ousley, B. Peterson, J. Piggot, C. Saulnier, M. State, W. Stone, J. Sutcliffe, C. Walsh, E. Wijsman. We thank the Allen Brain Atlas for use of their publicly available developing human brain expression data. Finally, we wish to thank Vlad Kustanovich (AGRE) for helping with access to ADOS severity score data, Dan Arking for sharing DNA from the SSC for Taqman genotyping, Samantha Maragh for zebrafish cDNA libraries and *eef1a1l1* primers, Ashish Kapoor for extensive discussions, Qian Jiang for translation of the He et al. publication, and Jill A. Rosenfeld, Lisa G. Shaffer, Yiping Shen, and Bai-Lin Wu for sharing copy number variant datasets. Sequencing services were provided by the Johns Hopkins University Next Generation Sequencing Center, Sidney Kimmel Comprehensive Cancer Center, Illumina Sequencing Services (Hayward, CA), and, the Johns Hopkins University Genetic Resources Core Facility. E.C.O. is a NARSAD young investigator. N.K. is a Distinguished George W. Brumley Professor. This work was funded by grants from the Simons Foundation to A.C. and to N.K., NIMH grant MH095867 to M.E.T., NIMH grants 5R25MH071584-07 and MH19961-14 to D.M.D.L. (Malison), NIMH grant R01MH081754 to A.C., and an Autism Speaks Dennis Weatherstone pre-doctoral fellowship (#7863) to T.T.

References

1. Kogan MD, et al. Prevalence of parent-reported diagnosis of autism spectrum disorder among children in the US, 2007. Pediatrics. 2009; 124:1395–1403.10.1542/peds.2009-1522 [PubMed: 19805460]
2. Jorde LB, et al. Complex segregation analysis of autism. American journal of human genetics. 1991; 49:932–938. [PubMed: 1928098]
3. Abrahams BS, Geschwind DH. Advances in autism genetics: on the threshold of a new neurobiology. Nature reviews. Genetics. 2008; 9:341–355.10.1038/nrg2346
4. Ronemus M, Iossifov I, Levy D, Wigler M. The role of de novo mutations in the genetics of autism spectrum disorders. Nature reviews. Genetics. 2014; 15:133–141.10.1038/nrg3585
5. Carter CO. Genetics of common disorders. British medical bulletin. 1969; 25:52–57. [PubMed: 5782759]
6. Chakravarti A. 2013 William Allan Award: My multifactorial journey. American journal of human genetics. 2014; 94:326–333.10.1016/j.ajhg.2013.11.014 [PubMed: 24607382]
7. Emison ES, et al. Differential contributions of rare and common, coding and noncoding Ret mutations to multifactorial Hirschsprung disease liability. American journal of human genetics. 2010; 87:60–74.10.1016/j.ajhg.2010.06.007 [PubMed: 20598273]
8. Arikkath J, et al. Delta-catenin regulates spine and synapse morphogenesis and function in hippocampal neurons during development. The Journal of neuroscience : the official journal of the Society for Neuroscience. 2009; 29:5435–5442.10.1523/jneurosci.0835-09.2009 [PubMed: 19403811]
9. Bareiss S, Kim K, Lu Q. Delta-catenin/NPRAP: A new member of the glycogen synthase kinase-3beta signaling complex that promotes beta-catenin turnover in neurons. Journal of neuroscience research. 2010; 88:2350–2363.10.1002/jnr.22414 [PubMed: 20623542]
10. Weiss LA, Arking DE, Daly MJ, Chakravarti A. A genome-wide linkage and association scan reveals novel loci for autism. Nature. 2009; 461:802–808.10.1038/nature08490 [PubMed: 19812673]
11. Talkowski ME, et al. Sequencing chromosomal abnormalities reveals neurodevelopmental loci that confer risk across diagnostic boundaries. Cell. 2012; 149:525–537.10.1016/j.cell.2012.03.028 [PubMed: 22521361]

12. Jho EH, et al. Wnt/beta-catenin/Tcf signaling induces the transcription of Axin2, a negative regulator of the signaling pathway. Molecular and cellular biology. 2002; 22:1172–1183. [PubMed: 11809808]
13. Itoh K, Sokol SY. Graded amounts of Xenopus dishevelled specify discrete anteroposterior cell fates in prospective ectoderm. Mechanisms of development. 1997; 61:113–125. [PubMed: 9076682]
14. Nojima H, et al. Genetic evidence for involvement of maternally derived Wnt canonical signaling in dorsal determination in zebrafish. Mechanisms of development. 2004; 121:371–386.10.1016/j.mod.2004.02.003 [PubMed: 15110047]
15. Lu Q, et al. delta-catenin, an adhesive junction-associated protein which promotes cell scattering. The Journal of cell biology. 1999; 144:519–532. [PubMed: 9971746]
16. Penzes P, Cahill ME, Jones KA, VanLeeuwen JE, Woolfrey KM. Dendritic spine pathology in neuropsychiatric disorders. Nature neuroscience. 2011; 14:285–293.10.1038/nn.2741 [PubMed: 21346746]
17. Kim H, et al. Delta-catenin-induced dendritic morphogenesis. An essential role of p190RhoGEF interaction through Akt1-mediated phosphorylation. The Journal of biological chemistry. 2008; 283:977–987.10.1074/jbc.M707158200 [PubMed: 17993462]
18. Israely I, et al. Deletion of the neuron-specific protein delta-catenin leads to severe cognitive and synaptic dysfunction. Current biology : CB. 2004; 14:1657–1663.10.1016/j.cub.2004.08.065 [PubMed: 15380068]
19. Matter C, Pribadi M, Liu X, Trachtenberg JT. Delta-catenin is required for the maintenance of neural structure and function in mature cortex in vivo. Neuron. 2009; 64:320–327.10.1016/j.neuron.2009.09.026 [PubMed: 19914181]
20. Abu-Elneel K, et al. A delta-catenin signaling pathway leading to dendritic protrusions. The Journal of biological chemistry. 2008; 283:32781–32791.10.1074/jbc.M804688200 [PubMed: 18809680]
21. Wang M, Dong Q, Zhang D, Wang Y. Expression of delta-catenin is associated with progression of human astrocytoma. BMC cancer. 2011; 11:514.10.1186/1471-2407-11-514 [PubMed: 22151302]
22. Rodova M, Kelly KF, VanSaun M, Daniel JM, Werle MJ. Regulation of the rapsyn promoter by kaiso and delta-catenin. Molecular and cellular biology. 2004; 24:7188–7196.10.1128/mcb.24.16.7188-7196.2004 [PubMed: 15282317]
23. Kim SW, et al. Non-canonical Wnt signals are modulated by the Kaiso transcriptional repressor and p120-catenin. Nature cell biology. 2004; 6:1212–1220.10.1038/ncb1191 [PubMed: 15543138]
24. Koutras C, Lessard CB, Levesque G. A nuclear function for the presenilin 1 neuronal partner NPRAP/delta-catenin. Journal of Alzheimer's disease : JAD. 2011; 27:307–316.10.3233/jad-2011-110536 [PubMed: 21811021]
25. Zhang J, et al. Isoform- and dose-sensitive feedback interactions between paired box 6 gene and delta-catenin in cell differentiation and death. Experimental cell research. 2010; 316:1070–1081.10.1016/j.yexcr.2010.01.006 [PubMed: 20074565]
26. Umeda T, et al. Evaluation of Pax6 mutant rat as a model for autism. PloS one. 2010; 5:e15500.10.1371/journal.pone.0015500 [PubMed: 21203536]
27. Davis LK, et al. Pax6 3′ deletion results in aniridia, autism and mental retardation. Human genetics. 2008; 123:371–378.10.1007/s00439-008-0484-x [PubMed: 18322702]
28. Duparc RH, Boutemmine D, Champagne MP, Tetreault N, Bernier G. Pax6 is required for delta-catenin/neurojugin expression during retinal, cerebellar and cortical development in mice. Developmental biology. 2006; 300:647–655.10.1016/j.ydbio.2006.07.045 [PubMed: 16973151]
29. Pinto D, et al. Functional impact of global rare copy number variation in autism spectrum disorders. Nature. 2010; 466:368–372.10.1038/nature09146 [PubMed: 20531469]
30. Medina M, Marinescu RC, Overhauser J, Kosik KS. Hemizygosity of delta-catenin (CTNND2) is associated with severe mental retardation in cri-du-chat syndrome. Genomics. 2000; 63:157–164.10.1006/geno.1999.6090 [PubMed: 10673328]

31. Vrijenhoek T, et al. Recurrent CNVs disrupt three candidate genes in schizophrenia patients. American journal of human genetics. 2008; 83:504–510.10.1016/j.ajhg.2008.09.011 [PubMed: 18940311]
32. Zhou J, et al. Presenilin 1 interaction in the brain with a novel member of the Armadillo family. Neuroreport. 1997; 8:2085–2090. [PubMed: 9223106]
33. Fujita T, et al. Delta-catenin/NPRAP (neural plakophilin-related armadillo repeat protein) interacts with and activates sphingosine kinase 1. The Biochemical journal. 2004; 382:717–723.10.1042/bj20040141 [PubMed: 15193146]
34. Martinez MC, Ochiishi T, Majewski M, Kosik KS. Dual regulation of neuronal morphogenesis by a delta-catenin-cortactin complex and Rho. The Journal of cell biology. 2003; 162:99–111.10.1083/jcb.200211025 [PubMed: 12835311]
35. Silverman JB, et al. Synaptic anchorage of AMPA receptors by cadherins through neural plakophilin-related arm protein AMPA receptor-binding protein complexes. The Journal of neuroscience : the official journal of the Society for Neuroscience. 2007; 27:8505–8516.10.1523/jneurosci.1395-07.2007 [PubMed: 17687028]
36. Laura RP, et al. The Erbin PDZ domain binds with high affinity and specificity to the carboxyl termini of delta-catenin and ARVCF. The Journal of biological chemistry. 2002; 277:12906–12914.10.1074/jbc.M200818200 [PubMed: 11821434]
37. Kim K, et al. Dendrite-like process formation and cytoskeletal remodeling regulated by delta-catenin expression. Experimental cell research. 2002; 275:171–184.10.1006/excr.2002.5503 [PubMed: 11969288]
38. Daniel JM, Reynolds AB. The catenin p120(ctn) interacts with Kaiso, a novel BTB/POZ domain zinc finger transcription factor. Molecular and cellular biology. 1999; 19:3614–3623. [PubMed: 10207085]
39. Yoon HG, Chan DW, Reynolds AB, Qin J, Wong J. N-CoR mediates DNA methylation-dependent repression through a methyl CpG binding protein Kaiso. Molecular cell. 2003; 12:723–734. [PubMed: 14527417]
40. Brigidi GS, et al. Palmitoylation of delta-catenin by DHHC5 mediates activity-induced synapse plasticity. Nature neuroscience. 2014; 17:522–532.10.1038/nn.3657 [PubMed: 24562000]
41. De Rubeis S, et al. CYFIP1 coordinates mRNA translation and cytoskeleton remodeling to ensure proper dendritic spine formation. Neuron. 2013; 79:1169–1182.10.1016/j.neuron.2013.06.039 [PubMed: 24050404]
42. Matsuoka RL, et al. Class 5 transmembrane semaphorins control selective Mammalian retinal lamination and function. Neuron. 2011; 71:460–473.10.1016/j.neuron.2011.06.009 [PubMed: 21835343]
43. Geschwind DH, et al. The autism genetic resource exchange: a resource for the study of autism and related neuropsychiatric conditions. American journal of human genetics. 2001; 69:463–466.10.1086/321292 [PubMed: 11452364]
44. Homer N, Merriman B, Nelson SF. BFAST: an alignment tool for large scale genome resequencing. PloS one. 2009; 4:e7767.10.1371/journal.pone.0007767 [PubMed: 19907642]
45. Li H, Durbin R. Fast and accurate long-read alignment with Burrows-Wheeler transform. Bioinformatics (Oxford, England). 2010; 26:589–595.10.1093/bioinformatics/btp698
46. McKenna A, et al. The Genome Analysis Toolkit: a MapReduce framework for analyzing next-generation DNA sequencing data. Genome research. 2010; 20:1297–1303.10.1101/gr.107524.110 [PubMed: 20644199]
47. Wang K, Li M, Hakonarson H. ANNOVAR: functional annotation of genetic variants from high-throughput sequencing data. Nucleic acids research. 2010; 38:e164.10.1093/nar/gkq603 [PubMed: 20601685]
48. Brewer GJ. Serum-free B27/neurobasal medium supports differentiated growth of neurons from the striatum, substantia nigra, septum, cerebral cortex, cerebellum, and dentate gyrus. Journal of neuroscience research. 1995; 42:674–683.10.1002/jnr.490420510 [PubMed: 8600300]

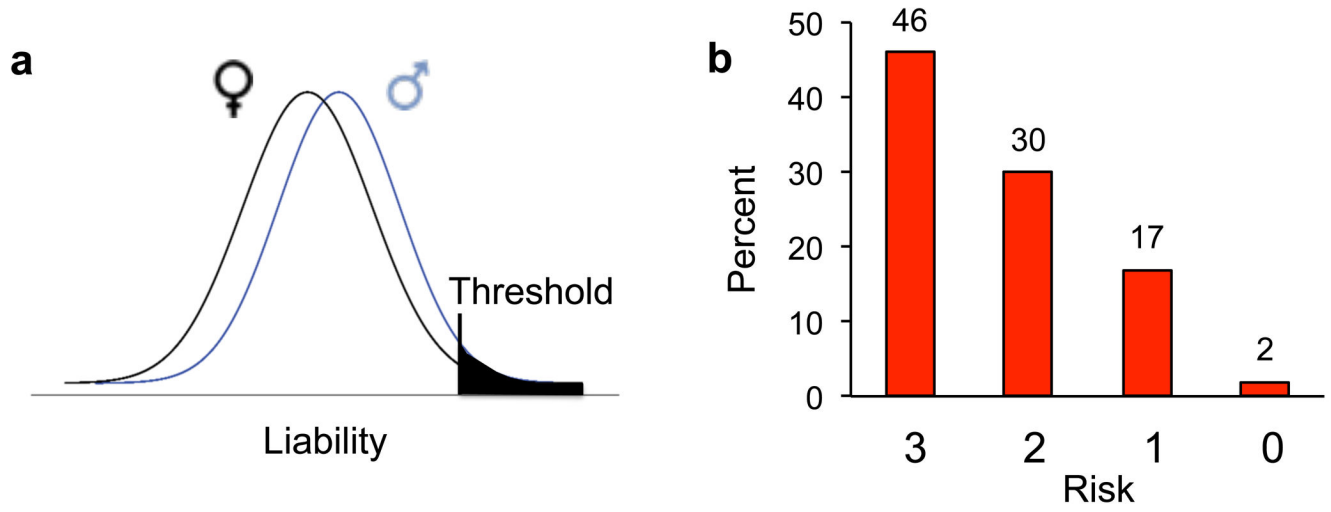

Figure 1. Genetic features of a sex-dependent multifactorial model

(a) Hypothetical sex-dependent liability distributions for autism under a multifactorial model of inheritance with a fixed biological threshold for affection. (b) Percent of Hirschsprung disease patients with damaging coding mutations within different risk classes characterized by gender, segment length, and familiality. The risk class is labeled 3,2,1,0 and is an additive score based on the number of factors with higher risk (female, long segment, multiplex) and comprise 13, 46, 60 and 55 patients, respectively (proportion trend test, $P=3.1x10^{-6}$).

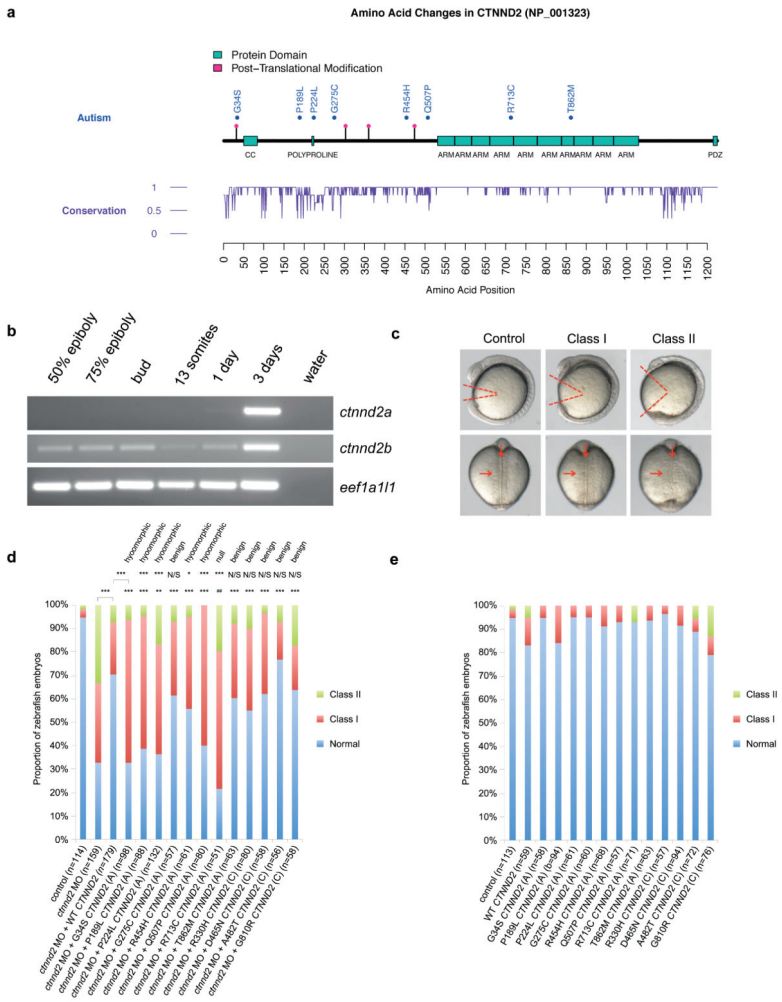

Figure 2. Missense variants in human delta catenin and their effect on protein function in vivo

(a) CTNND2 annotated with validated missense mutations in autism patients; G34S, G275C, Q507P, R713C, T862M variants are conserved to zebrafish. (b) Expression of two *CTNND2* zebrafish orthologs (*ctnnd2a*, *ctnnd2b*) in development. Aberrant phenotypes are observed with *ctnnd2b (*the only ortholog expressed at these gastrulation time points) morpholino (MO) knockdown only at key stages of gastrulation (50% epiboly, 75% epiboly, bud). Elongation factor alpha (*eef1a1l1*) is shown as a control for ubiquitous expression. (c) Representative lateral and dorsal images of Class I and Class II *ctnnd2b* morphants (2 ng MO) at the 8–10 somite stage reveal defective gastrulation movements. (d) Quantification of gastrulation phenotype in control, MO and rescue constructs: wild type, autism variants (G34S, P189L, P224L, G275C, R454H, Q507P, R713C, T862M), and control variants (R330H, D465N, A482T, G810R) are indicated. (e) Quantification of gastrulation phenotype in overexpression constructs: wild type, autism variants (G34S, P189L, P224L, G275C, R454H, Q507P, R713C, T862), and control variants (R330H, D465N, A482T, G810R) are indicated. Chi-square tests were conducted with *, ** and *** indicating $P < 0.05$, $P < 0.01$ and $P < 0.001$, respectively, and ## indicating no rescue and worse than MO alone ($P < 0.01$). Sample size (n) is marked for each condition.

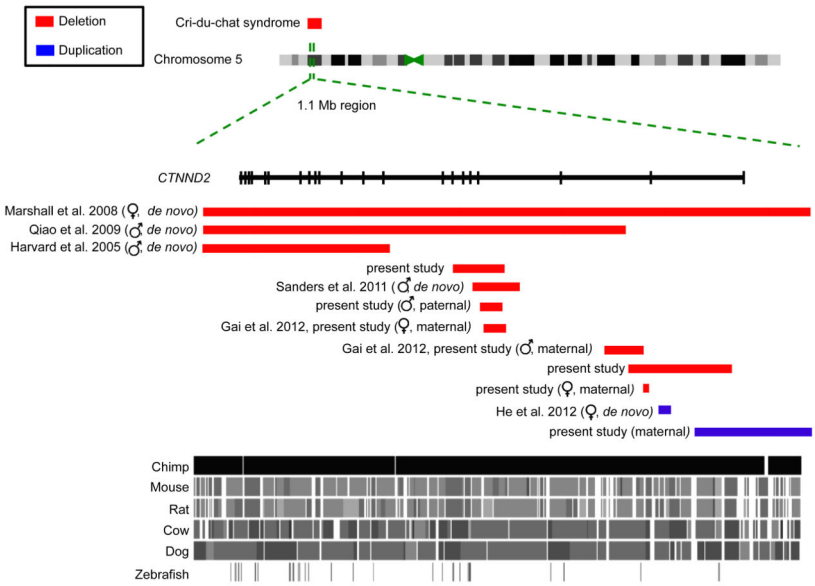

Figure 3. Copy number variants (CNV) in human CTNND2

CNVs at the 1.1 Mb *CTNND2 locus (chr5:10905332-12034584, hg19),* the chromosomal location, extent of each deletion and duplication, patient gender, parental origin and citation, are shown for each variant identified in autism patients and individuals with other neurodevelopmental disorders. Extensive genomic sequence conservation across the entire region in selected vertebrates is shown.

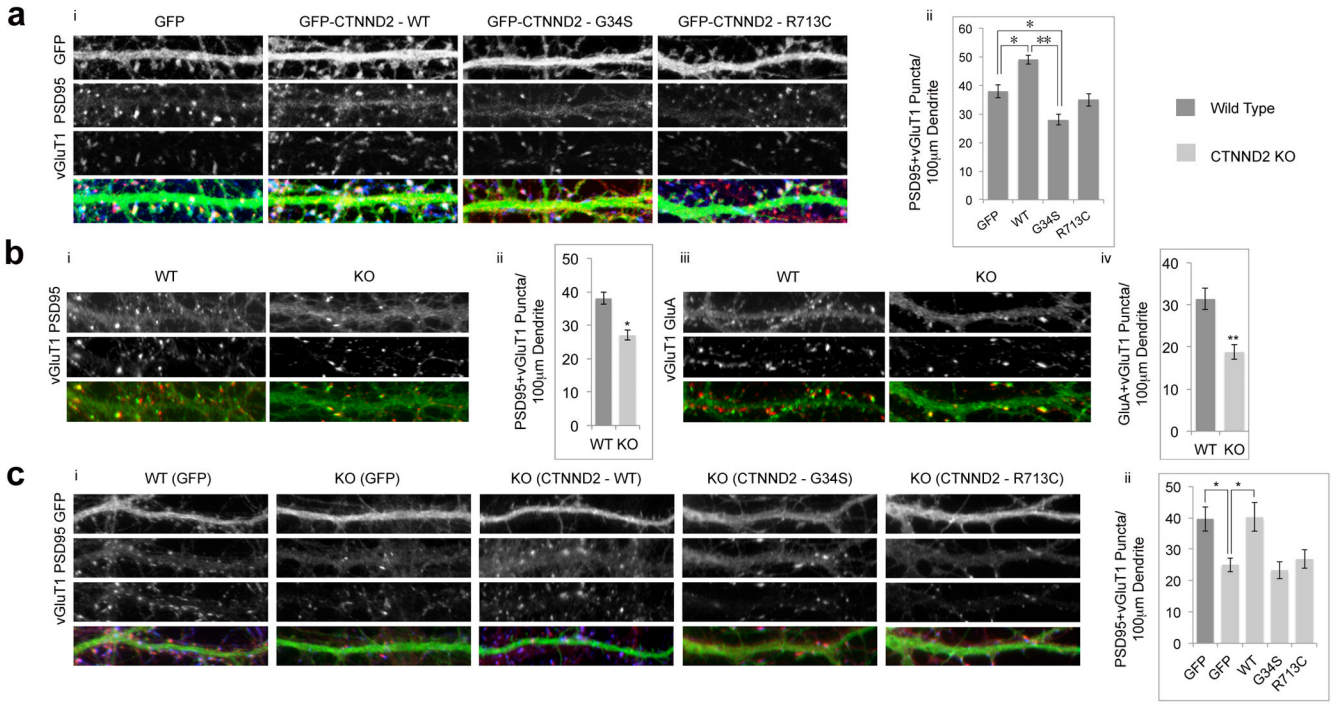

Figure 4. Delta catenin is critical for maintaining functional neuronal networks

(a) Gain of function: (i) Over expression of *CTNND2* leads to an increase in the number of excitatory synapses. Primary dendrites from neurons transfected with GFP alone, GFP fusion with wild type *CTNND2*, or mutant isoforms, and immunolabeled with vGluT1 and PSD95. (ii) Quantification of number of PSD95+vGluT1 positive puncta per 100 µm of dendritic length (N=12 each). (b) Loss of function: (i) Neurons from *Ctnnd2* null mutants have a significant reduction in synapse density. Synapses are identified as puncta with PSD95 and vGluT1 overlap. (ii) Quantification of the number of PSD95+vGluT1 positive puncta per 100 µm of dendritic length (N=13 each). (iii) Alternatively, neurons were immunolabeled with GluA and vGluT1 to identify active functional excitatory synapses. (iv) Quantification of the number of GluA+vGluT1 positive puncta per 100 µm of dendritic length (N=15 each). (c) Rescue of loss of function: (i) WT CTNND2 but not its mutant isoforms can rescue the loss of phenotype in neurons from CTNND2 null mutants. Primary dendrites from neurons transfected with GFP alone, GFP fusion with wild type CTNND2, or mutant isoforms, and immunolabeled with vGluT1 and PSD95. (ii) Quantification of the number of PSD95+vGluT1 positive puncta per 100 µm of dendritic length (N=14 each). Color used for merged panels are GFP (green) PSD95 (red), GluA (Red) and vGluT1 (blue). Student's t-test were conducted with * and ** represents P<.05 and P<.001, respectively. Error bars represent standard error of mean.

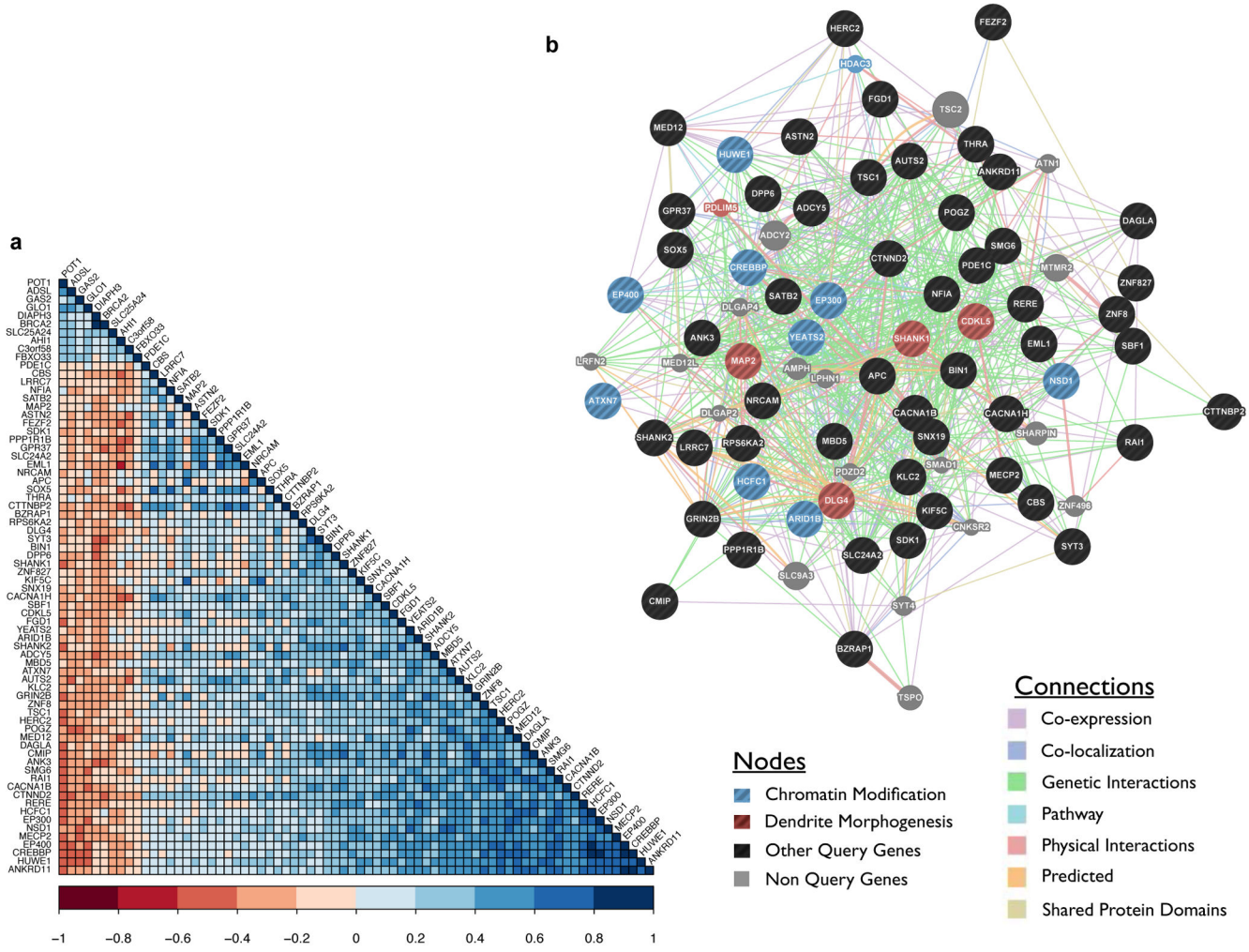

Figure 5. Gene expression correlation between CTNND2 and known autism genes

(a) Plot of all autism genes significantly (positive and negative) correlated with *CTNND2* in the developing human brain (microarray data from www.brainspan.org). (b) Pathway analysis of the autism genes positively correlated with delta catenin reveals significant enrichment of genes involved in chromatin modification and dendrite morphogenesis.